

Mangrove Mapping of Ratnagiri Coast using Different Classification Techniques

Ajay D. Nakhawa^{1*}, Sandip S. Markad¹, Priyanka S. Vichare² and Mangesh Shirdhankar³

- ¹ College of Fishery Science, Nagpur 440 001, India
- ² Central Marine Fisheries Research Institute, Regional Centre, Mumbai 400 061, India
- ³ College of Fisheries, Ratnagiri 415 629, India

Abstract

Mangrove coverage of Ratnagiri coast was mapped by using different techniques such as supervised classification, supervised classification of principal components, unsupervised classification and unsupervised classification of principal components and overall classification accuracy ranged from 79.46-86.19, 82-89, 84.52-89 and 89-93% respectively. The kappa co-efficient for supervised classification, supervised classification of principal components, unsupervised classification and unsupervised classification of principal components were 0.74-0.82, 0.78-0.86, 0.81-0.87 and 0.87-0.90 respectively. Overall classification accuracy achieved by unsupervised classification of principal components technique was comparatively better than overall classification accuracy achieved by other techniques. Thus this technique is found appropriate for mapping the mangrove coverage in the Ratnagiri block.

Keywords: Mangrove, supervised classification, unsupervised classification, PCA

Received 25 February 2012; Revised 15 May 2012; Accepted 10 August 2012

Introduction

Remote sensing technique emerges as a valuable tool for fast, efficient and accurate means of information retrieval to detect cause, extent and modification of structural changes over time. Information gained can be utilized for effective planning and management of mangrove forests (Vijay et al., 2005). Conventional methods such as stratified, multi-phase, double-phase and quadratics sampling methods were used for assessment of mangrove forests (Anon, 1994). Field data requirement of conventional methods was huge and expensive in terms of time, labour as well as funds. Therefore, these methods are not used widely at present. On the other hand, orbital remote sensing provides synoptic views, which are very useful in monitoring and assessment of mangrove vegetation. Synoptic views of an area retrieved through repetitive and multi-spectral remote sensing data, can be useful for monitoring coastal vegetation. Vegetation has different optical properties in the visible, near infrared (NIR) and middle infrared (MIR) region. These optical properties are important for discriminating mangrove vegetation type and also to certain extent for species identification (Nayak & Bahuguna, 2001). Jagatap et al. (2001) assessed coastal wetland resources of the central west coast, Goa and Maharashtra of India by using Landsat data of 1985-86 and Survey of India (SOI) topographical maps at scale 1:2 50 000 as ancillary data. Nayak & Bahuguna (2001) extensively used Indian remote sensing satellite (IRS) data for monitoring mangrove and coastal vegetation for the entire coastline of India. Restoration of Pichavaram mangrove forest by comparing satellite data of Landsat TM and IRS 1D LISS III was studied by Selvam et al. (2003). Vijay et al. (2005) mapped mangroves and detected changes in mangroves around the Mumbai coast by using remote sensing data. Ramasubramanian et al. (2006) studied mangroves of Godavari through analysis of multi-temporal and multi-spectral satellite data of Landsat TM and IRS 1D LISS III. Majority of the coastal community, especially the fishers are traditionally dependent on mangroves for their domestic needs. They provide large amount of resources but have been under threat due to

¹ Present Address National Institute of Abiotic Stress Management, Baramati - 413 115, India

^{*} E-mail: ajaynakhawa@hotmail.com

anthropogenic activities such as agriculture, urbanization and industrialization. The change in atmospheric temperature may alter precipitation pattern and thus cause salinity stress, which will affect the growth and survival of mangroves and rise in sea level will shift the mangrove habitat towards land (Daniel, 2007), with limited land margin having no scope for further expansion. Classification of mangrove vegetation is vital for a proper mangrove management plan. No such management measures are followed due to lack of information on mangrove areas at regional level. So it is important to have information regarding mangrove environment at national as well as regional level. An attempt is made in the present study to map mangrove in Ratnagiri block by using different remote sensing techniques.

Materials and Methods

Study area: Study was carried out along the coastline of Ratnagiri block situated between 17°18′50.89" N latitude and 73°11′15.90" E longitude to 16°45′37.70" N latitude and 73°18′20.00" E longitude. Along with mangroves different natural features present in the vicinity of coastline was also observed for better discrimination of the mangroves areas. The geographical location of study area is shown in Fig.1.

Satellite images and image processing: Temporal satellite images of different sensors were used for mapping of study area. The satellite images of Landsat- Multi-Spectral Scanner (MSS), Thematic Mapper (TM) and Enhanced Thematic Mapper plus (ETM+) were used. TERRA Advances Spaceborne Thermal Emission and Reflection Radiometer (ASTER) satellite images were obtained from Earth Resources Observation and Sciences, USGS. Digital satellite image of IRS P6 Linear Imaging Self Scanner (LISS) III was procured from National Remote Sensing Center (NRSC), Hyderabad. The ERDAS Imagine 9.1 software was used for carrying out image processing of different satellite images.

Ground control points and field data: Ground control points (GCPs) were collected through handheld e-trex Garmin GPS, receiver was set to Universal Transverse Mercator (UTM) projection with World Geodetic System 1984 (WGS84) datum and accuracy was 1-5 meter with DGPS correction. GCPs such as road to road intersection, road to railway crossing, end points of jetties, runways,

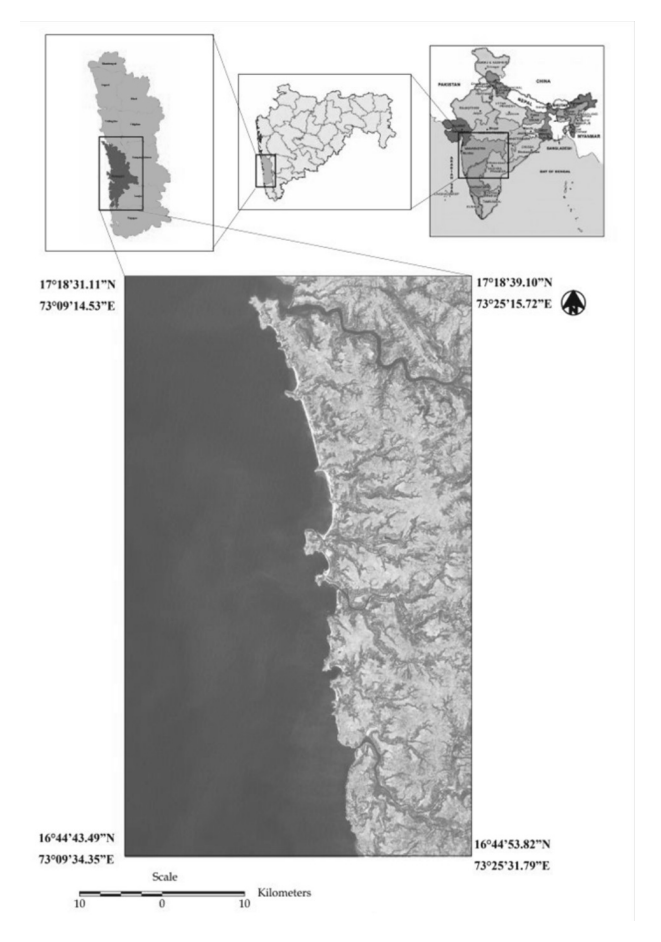


Fig. 1. Map showing study area

bridge and bunds which were easy to locate on the satellite image as well as on ground were identified. The geographical locations of mangrove area along with other coastal features were collected by field survey to confirm the estimated result by remote sensing techniques.

Image preprocessing: The preprocessing was applied to the digital satellite data so as to have correct satellite image for extracting shoreline changes. The raw digital satellite image data was first transformed into image format by importing into ERDAS image processing system.

Geometric corrections: The satellite images were rectified to the proper geometric projection with minimum of Root Mean Square (RMS) to attain appropriate accuracy before image processing. For application of geometric corrections, geo-coded image of ASTER (B3b) was first corrected for geometric errors using GCPs. This geometrically corrected image was then used as reference image

for geometric enhancements of other multi-spectral satellite images through image geo-referencing and images were rectified to UTM (Zone 43) map projection with RMS error threshold of 0.5 pixels.

Radiometric correction: Geometrically corrected images were then processed to convert Digital Number (DN) values of image pixels to Top-of-Atmosphere (TOA) reflectance values, for which DN values were first converted to absolute radiance values measured at sensor using following expression-

$$L = L_{MIN} + \frac{L_{MAX} - L_{MIN}}{255} \times DN$$

Where,

L = Spectral radiance measured at sensor (mW cm⁻² Sr⁻¹),

LMAX = Maximum radiance measured at sensor $(mW cm^{-2} Sr^{-1})$,

LMIN = Minimum radiance measured at sensor (mW cm⁻² Sr⁻¹),

DN = Calculated digital number value of image pixels (0 to 255)

At sensor radiance values were converted to TOA reflectance values by the following expression-

$$R = \frac{\pi x L x d^2}{ESUN\lambda x \cos\theta_c}$$

Where,

R = TOA Reflectance,

 $\pi = 3.414593,$

L = Spectral radiance measured at sensor (mW cm⁻² Sr⁻¹),

d = Earth – Sun distances in astronomical units,

ESUN = Mean solar exo-atmospheric spectral irradiance $[W/(m^2 \mu m)]$,

 θ s = Solar zenith angle (°).

Conversion of calculated DN values to TOA reflectance values aided the reduction of radiometric errors associated with variations in the radiation due to seasonal variations and atmosphere. In addition to this, TOA reflectance values represented the ratio of radiance recorded at the satellite sensor against the irradiance from the sun. This provided a standardized measure for direct comparison of digital image data used in present study, which was acquired by different sensors onboard different satellites.

Resolution merging: The multi-spectral satellite images used were with varying spatial resolutions because of which the extraction of shoreline and associated changes was difficult. Therefore, all images were transformed to equal high spatial resolution by merging them with single date high spatial resolution imagery with 15 m spatial resolution using multiplication method. The transformation was based on following mathematical expression-

$$DN_O = DN_M \times DN_H$$

$$DN_O = DN_M \times 1$$

$$DN_O = DN_M$$

Where,

 DN_O = Pixel value of output merged image,

 DN_{M} = Pixel value of multi-spectral image,

 DN_H = Pixel value of high spatial resolution image

The pixel values of images should remain unchanged if those are multiplied with images with pixel value of one. Therefore, a reference image with 15 m spatial resolution was generated by assigning pixel value of one to all the pixels of visible band of ASTER (B3b). This imagery was then used for transforming all the images to 15 m spatial resolution without altering spectral information.

Image subset: The area of interest was extracted from the preprocessed full scene images using subset module of the ERDAS Imagine software. Subsets with Area of interest (AOI) were drawn from the complete study area with the help of ERDAS Imagine software.

Image processing: Different digital image processing techniques were applied to preprocessed images of Landsat TM, Landsat ETM, ASTER and IRS P6 LISS III for mapping the mangrove area from 1989-2009. Prior to classification land cover classes were defined as mangrove, vegetation, exposed land, mudflats, sand and water. In some techniques mudflat was confused with exposed land, so mudflat class was merged with exposed land to reduce the error in classification. The classification was carried out by using all bands of satellite images, except thermal band of ASTER and Landsat. The images were processed in two steps, initially the satellite images were classified simply by using the supervised and unsupervised techniques whereas, in

second step satellite images were enhanced through Principal Component Analysis (PCA) and classified using unsupervised and supervised classification techniques. The classified maps were evaluated by accuracy assessment of all the land cover classes through error matrix and *kappa co-efficient*.

Supervised classification: The supervised classification of multi-spectral images and PCA transformed images was performed using the Maximum Likelihood Classifier. The first four bands of PCA were used for the supervised classification (Omo-Irabor & Oduyemi, 2007). The adequate spectral signatures for different land cover classes were taken by employing signature editor. The spectral signature for different land cover classes was selected based on field data and reference images. The classes belonging to same land cover class were merged to make five distinct land cover classes. The interim result showed some isolated pixels; so to reduce the error, fuzzy convolution of 5x5 pixel window was performed. After fuzzy convolution, isolated pixels were effectively eliminated as well as spatial continuity of the classes were preserved.

Unsupervised classification: The Iterative Self Organizing Data Analysis (ISODATA) algorithm was used to classify the spectral cluster of multispectral and PCA transformed images. Minimum Spectral Distances capability of ISODATA algorithm was used to assign as cluster for potential pixels. The trial and error method was performed for optimizing the number of clusters, convergence threshold and number of iteration so as to get distinct differentia between mangroves and other land cover classes. The opacity of all clusters was set to zero, which resulted in disappearance of image. Then cluster labeling was done by setting opacity to one so as to make images visible. The cluster that appears was compared with reference image and field data to assign label. Labeling of particular cluster was carried out by assigning a distinct color depending upon landcover class. The classes belonging to same landcover class were fused through recoding, to make five distinct land cover classes.

The accuracy of the classified images was tested using the error matrix. The classified pixels were cross checked with the test sample obtained from field data for assessing the accuracy of the classified thematic maps. Overall accuracy as well as user and producer accuracy were determined for each classified thematic maps, while errors of omission

and commission were also estimated for each landcover class (Lillesand et al., 2004). The *Kappa* co-efficient was calculated separately for each error matrix. The overall classification accuracy of different techniques was tested by chi-square test (Snedecor & Cochran, 1967).

Results and Discussion

The RMS values recorded during image georectification of different satellite image data used in the present study ranged from 0.1910 to 0.3255 pixels. Omo-Irabor & Oduyemi (2007) reported RMS value of 0.5 pixel for Landsat TM and ETM+ during the study of landcover changes in the Niger delta. Gao (1999) reported RMS in the range of 0.828-1.001 pixels for SPOT XS data during mangrove mapping in Newzealand. The RMS errors reported by them were much higher than that recorded during the present study, ensuring higher precisions in mangrove mapping and change analysis estimation of the present study.

Studies hitherto reported have used various remote sensing classification techniques such as supervised classification (Kristine,1983; Satapathy et al., 2007), supervised classification of principal components (Green et al., 1998), unsupervised classification (Godstime et al., 2007; Mimi et al., 2007) and unsupervised classification of principal components (Gluck et al., 1996) to classify the mangroves. In the present study mangrove were classified using these techniques to understand variations due to processing techniques used to classify the mangrove The overall accuracies achieved for coverage. different techniques viz., supervised and unsupervised classification of multispectral images as well as supervised and unsupervised classification of PCA transformed images range from 79.46-86.19, 82-89, 84.52-89 and 89-93% respectively. Though the values of overall accuracy achieved by unsupervised classification of principal component were higher, the chi-square test did not reveal significant differences (p>0.05) among the correctly classified pixels recorded through various classification techniques.

The overall accuracies of 79.73, 81, 86.19 and 79.46% were achieved during the supervised classification of Landsat-TM, ETM+, ASTER and LISS III respectively. In supervised classification of principal components transformed images, the overall accuracy obtained were 82, 85, 89 and 85% for Landsat-TM,

ETM+, ASTER and LISS III respectively. Overall classification accuracy as reported by Kristine (1983) for supervised classification of Landsat TM data was 74%. As compared to this value, overall classification accuracy recorded in the present study for supervised classification was higher in all the satellite images. Satapathy et al. (2007) have reported overall classification accuracy for supervised classification of IRS P6 LISS III as 90%, which was comparatively much higher than overall classification accuracy achieved after processing LISS III in the present study. The overall classification accuracy after supervised classification of principal components with Landsat TM data was 92% as reported by Green et al. (1998) and which was much higher than overall classification accuracy recorded during the present study with any of the satellite image data set. It was interesting to note that the supervised classification after principal component analysis could distinctly distinguish mud flats as well as water. Inspite of this, the technique was adopted by very few workers (Stacy & Marvin, 2002).

The overall classification accuracies achieved for unsupervised classification of Landsat-TM, ETM+, ASTER and LISS III were 84.52, 86, 89 and 86.43% respectively while the unsupervised classification of principal component transformed images of Landsat-TM, ETM+, ASTER and LISS III revealed the overall accuracies of 89, 90, 93 and 90% respectively. Similarly overall classification accuracies for Landsat TM and ETM+ as reported by Godstime et al. (2007) ranged from 89-95 and 91-95% respectively, which were relatively more than that was recorded during the present study. Mimi et al. (2007) have claimed the overall classification accuracy of 86.7% for ASTER by using the ISODATA unsupervised classification, which was comparatively lower than overall classification accuracy recorded for ASTER image data in the present study. In the present study, overall classification accuracies recorded for unsupervised classification of principal components of different satellite images ranged from 89 to 93%. The overall classification accuracy after classification of principal components with Landsat TM data was 81% as reported by Gluck et al. (1996), which was comparatively lower than overall classification accuracies recorded during the present study with any of the satellite images.

In supervised classification of multispectral images, an average error of omission was 26.25%, average error of commission was 12.12% while the average

error of omission and commission of 14.06 and 10.30% respectively were committed during supervised classification of principal component transformed images. In this technique most of pixels eliminated from mangrove class were incorporated in vegetation, exposed land, water as well as mudflats and pixels incorporated in mangrove class were frequently from vegetation, mudflats as well as water. Errors of omission and commission for mangrove classes were more, when processed with supervised classification techniques, while those were reduced in data processed with supervised classification of principal components. Therefore, it is always better to perform principal components analysis prior supervised classification for improvement in classification accuracy.

The average error of omission and commission that occurred during unsupervised classification of multispectral images were 22.5 and 8.13% respectively, whereas the average error of omission and commission that occurred during unsupervised classification of principal component transformed images were 13.12 and 5.38% respectively. During unsupervised classification of multispectral images, the pixels expelled from the mangrove class were integrated in vegetation, exposed land and mudflat except in ASTER image. In ASTER image, pixels expelled from mangrove class were included in mudflats and vegetation classes due to spectral mixing of mangrove, mudflats and vegetation at the border of the mangrove forest. In mangroves toward seaward side, some pixels were incorporating mangrove and mudflats, while toward landward side some pixels were incorporating mangrove and terrestrial vegetation. Similarly, pixels excluded from mangrove class in LANDSAT TM and ETM+ images were mostly from vegetation, exposed land and mudflats. The pixels incorporated in LISS III image was mainly from vegetation, sand, mudflats and water. The error of omission and commission that occurred in unsupervised classification of principal component transformed image were with only two classes viz., vegetation and mudflats. These errors could have occurred because, toward landward side mangrove was bordered by terrestrial vegetation such as coconut, mango and marsh vegetation. Moreover, human encroachment in low lying areas near mangrove forests resulted in conversion of some mangrove areas into agriculture or horticultural lands. So there were chances of spectral mixing within mangroves and other vegetation type near bordering pixels. Further, there were chances of spectral mixing in spare mangrove patches and bordering area of mangroves with mudflats as these mudflats were prime area of mangrove development.

The present study showed distinct segregation of mudflats after unsupervised classification of satellite images, while in supervised classification it was only possible after transformation of satellite images in to principal components. Reduction of errors of omission and commission was observed, when unsupervised classification of principal components was performed. In unsupervised classification, errors of omission and commission occurred with vegetation, mudflat and exposed land whereas, in unsupervised classification of principal components it occurred with only vegetation and mudflats. Unsupervised classification of principal components revealed enhanced overall classification as well as appropriate classification of mangroves as compared to simple unsupervised classification.

Different approaches of classification techniques did not reveal substantial difference, but variation in enhancement of overall mangrove classification accuracy was observed, when satellite images were classified with supervised or unsupervised technique after transformation into principal components.

References

- Anon (1994) Mangrove Forest Management Guidelines. FAO Forestry Paper No. 117
- Chaichoke, V., Andrew, K. S. and Willem, F. B. (2006) A post-classifier for mangrove mapping using ecological data. ISPRS. J. Photogramm. 61: 1-10
- Daniel, M. A. (2007) Mangrove forests: Reilience, protection form tsunamis, and responses to global climate change. Estuar. Coast. Shelf. Sci. 76: 1-13
- Gao, J. (1999) A comparative study on spatial and spectral resolutions of satellite data in mapping mangrove forest. Int. J. Remote. Sens. 20 (14): 2823-2833
- Gluck, M., Rempal, R. and Uhig, P.W.C. (1996) An evaluation of remote sensing for regional wetland mapping application. Forest Research Report No. 137. 33 p, Ontario Forest Research Institute Sault Ste Marie, Ontario, Canada
- Godstime, K. J., Jimy, O. A., Ekechukwu, S., Peter, N. and Joseph, A. (2007) Satellite-based assessment of the extent and changes in the mangrove ecosystem of the Niger delta. Mar. Geod. 30: 249-267

- Green, E. P., Clark, C. D., Mumby, P. J., Edwards, A. J. and Ellis, A. C. (1998) Remote sensing technique for mangrove mapping. Int. J. Remote. Sens. 19 (5): 935-956
- Jagatap, T. G., Naik, S. and Nagle, V. L. (2001) Assessment of coastal wetland resources of central west coast, India, using Landsat data. JISRS. 29 (3): 140-150
- Kristine, M. B. (1983) Remote sensing of wetlands. IEEE. Trans. Geosci. Remote. Sens. GE-21 (3): 383-392
- Lillesand, T. M., Kiefer, R. W. and Chipman, J. W. (2004) Remote Sensing and Image Interpretation, 763 p, 5th edn., John Wiley & Sons (Asia) Pte. Ltd., Singapore
- Mimi, D., Stacky, D. J., Susan, A. C. and Donald, C. P. (2007) Optimizing remote sensing and GIS tools for mapping and managing the distributions of an Invasive mangrove (*Rhizophora mangle*) on south Molokai, Hawaii. Mar. Geod. 30: 125-144
- Nayak, S. and Bahuguna, A. (2001) Application of remote sensing data to monitor mangrove and other coastal vegetation of India. Indian. J. Mar. Sci. 30 (4): 195-213
- Omo-Irabor, O. O. and Oduyemi, K. A. (2007) Hybrid image classification approach for the systematic analysis of land cover (LC) changes in the Niger delta region. *ISSDQ*, Conferences proceedingsessions,http.//www.itc.nl ISSDQ2007/proceeding session 02 html (Accessed 08 August 2008)
- Ramasubramanian, R., Gnanappazham, L., Ravishankar, T. and Muniyammal, N. (2006) Mangrove of Godavarianalysis through remote sensing approach. Wetlands. Ecol. Manage. 14: 29-37
- Satapathy, D. R., Krupadam, R. J., Pawan, K. and Wate, S. R. (2007) The application of satellite data for the quantification of mangrove loss and coastal management in the Godavari estuary, East coast of India. Environ. Pollut. Control. 134: 453-469
- Selvam, V., Ravichandran, K. K., Gnanappazham, L. and Navamuniyammal, M. (2003) Assessment of community-based restoration of Pichvaram mangrove wetland using remote sensing data. J. Curr. Sci. 85 (6): 794-798
- Snedecor, G. W. and Cochran, W. G. (1967) Statistical Methods, 6th edn., 593 p, Oxford and IBH Publishing Co., New Delhi, India
- Stacy, L. O. and Marvin, E. B. (2002) Satellite remote sensing of wetlands. Wetlands. Ecol. Manage. 10: 381-402
- Vijay, V., Biradar, R. S., Inamadar, A. B., Deshmukh, G., Raj, S. and Madhavi P. (2005) Mangrove mapping and change detection around Mumbai (Bombay) using remote sensed data. Indian. J. Mar. Sci. 34 (3): 310-315